

# Synthesis and characterization of ionic Ru(III) complexes containing dimethylsulfoxide and dinitrogen heterocyclic ligands

Craig M. Anderson<sup>a,\*</sup>, Amnon Herman<sup>a</sup>, Fernande D. Rochon<sup>b</sup>

<sup>a</sup> Department of Chemistry, Bard College, P.O. Box 5000, Annandale-on-Hudson, NY 12504-5000, United States

<sup>b</sup> Département de chimie, Université du Québec à Montréal, CP 8888, Succ. Centre-Ville, Montréal, Québec, Canada H3C 3P8

Received 6 March 2007; accepted 30 March 2007

Available online 10 April 2007

## Abstract

Several new Ru(III) DMSO compounds including  $[\text{PPh}_4]\text{trans}[\text{Ru}(\text{DMSO})_2\text{Cl}_4]$ ,  $[\text{PPh}_4]\text{trans}[\text{Ru}(\text{DMSO})(\text{pyrazine})\text{Cl}_4]$  (**2**),  $[\text{PPh}_4]\text{trans}[\text{Ru}(\text{DMSO})(4,4'\text{-bipyridine})\text{Cl}_4]$  and  $[\text{PPh}_4]\text{trans}[\text{Ru}(\text{DMSO})(\text{pyrimidine})\text{Cl}_4]$  were reported and characterized. The crystal structure of **2** and its  $\text{Na}^+$  analogue were determined by X-ray diffraction methods. The  $\text{PPh}_4^+$  complex **2** is a discrete ionic compound, while the compound  $[\text{Na}]\text{trans}[\text{Ru}(\text{DMSO})(\text{pyrazine})\text{Cl}_4] \cdot \text{DMSO}$  (**3**) crystallized with a molecule of DMSO. The environment around the Na atom is a distorted octahedron with short contacts with three chloro ligands, two O atoms from the bonded and unbonded DMSO molecules, and the unbonded N atom of the pyrazine ligand. The Na atoms form bridges between the complexed anions in **3** resulting in the formation of infinite chains or ribbons parallel to the *b* axis. The chains are held together by van der Waals interactions. © 2007 Elsevier Ltd. All rights reserved.

**Keywords:** Ruthenium; DMSO; Pyrazine; Pyrimidine; 4,4-Bipyridine; Crystal structures; NMR; IR

## 1. Introduction

The anticancer drug *cisplatin*, *cis*- $\text{Pt}(\text{NH}_3)_2\text{Cl}_2$ , and a few other platinum agents are widely used in the clinical treatment of testicular, ovarian, bladder, head and neck tumors [1–3]. The clinical success of *cisplatin* has proved to be limited due to significant side effects and resistance that cause relapse [3]. Therefore, much interest has focused on developing new chemotherapeutic metal complexes with improved properties. Subsequent studies on many platinum-containing complexes have been performed [4–8]. However, most of these complexes have been proven to have the same or only slightly better efficacy than *cisplatin* [3].

For the past two decades, much work has focused on the synthesis and pharmacological evaluation of new compounds containing ruthenium centers [9–11]. A major rea-

son for this can be attributed to the reduced side effects of these complexes, due to their lower systemic toxicity. Complexes with ruthenium(III) centers have been synthesized and have demonstrated antitumor activity, as well as remarkable antimetastatic behavior [10,11]. It is speculated that ruthenium(III) complexes are reduced *in vivo* to the more labile ruthenium(II) and this is a major reason for its biological activity [9–11]. Due to lower oxygen and lower pH at tumor sites, ruthenium's "activation by reduction" process makes it very selective as the metal complex may accumulate in these hypoxic environments [12]. Only a small number of ruthenium(III) complexes have been found to be effective, with the best examples being:  $[\text{Na}]\text{trans}[\text{RuCl}_4(\text{DMSO})(\text{Im})]$  [13], NAMI, its imidazolium analogue  $[\text{ImH}]\text{trans}[\text{RuCl}_4(\text{DMSO})(\text{Im})]$  [14], NAMI-A and the indazole compound  $[\text{IndH}]\text{trans}[\text{RuCl}_4(\text{Ind})_2]$  [15], KP1019. NAMI-A shows high selectivity for solid tumor metastases [16,17] and low toxicity at pharmacologically active doses and was found to effectively interfere with cell cycle regulation and angiogenesis [18–20]. The above properties have made NAMI-A the first

\* Corresponding author. Tel.: +1 845 758 7293.

E-mail address: [canderso@bard.edu](mailto:canderso@bard.edu) (C.M. Anderson).

ruthenium(III) compound to successfully complete phase I clinical trials [21]. The main feature of the majority of these complexes is the presence of four chlorides, one DMSO, and one N-donor ligand in the coordination sphere. At present, very few examples of such ruthenium(III) complexes exist that have been structurally characterized by X-ray diffraction methods. These include complexes, for example, where the N-donor ligand is ammonia [22], thiazole [23], guaninium [24], imidazole [22], pyridine [25], triazole [26] as well as symmetrical ruthenium dimers with pyrazine, pyrimidine, and bipyridine [27], and the unsymmetrical dimer with bridging pyrazine [28]. Here we report the synthesis and characterization of several ruthenium(III) complexes with dimethylsulfoxide and heterocyclic dinitrogen ligands as well as the crystal structures of the  $[\text{Ru}(\text{DMSO})(\text{pz})\text{Cl}_4]^-$  (pz = pyrazine) monoanion with two different cations, tetraphenylphosphonium ( $\text{PPh}_4$ ) and Na. These cations are quite different and the architectures of the crystal structures were expected to differ considerably. These two compounds are the first two Ru(III) species containing a terminal pyrazine ligand to be characterized structurally.

## 2. Experimental

Ethanol (100%) was purchased from Pharmaco Products Inc. All other reagents and solvents were purchased from Sigma Aldrich Inc. IR spectra were recorded in the solid state on a Nicolet 4700 FTIR spectrometer between 4000 and  $250\text{ cm}^{-1}$ .  $^1\text{H}$  NMR spectra were measured in  $\text{D}_2\text{O}$ , acetone- $d_6$ ,  $\text{CDCl}_3$ , and  $\text{CD}_3\text{CN}$  on a Varian Gemini 300 MHz spectrometer. The solvent peaks at 4.80 ppm, 2.05 ppm, 7.26 ppm, and 1.94 ppm for  $\text{D}_2\text{O}$ ,  $\text{CD}_3\text{COCD}_3$ ,  $\text{CDCl}_3$ , and  $\text{CD}_3\text{CN}$ , respectively, were used as internal standards for the  $^1\text{H}$  NMR spectra. Spectral abbreviations used below: br (broad), vbr (very broad), s (strong), m (medium), w (weak), sh (shoulder).

### 2.1. Synthesis

$[(\text{DMSO})_2\text{H}]\text{trans}-[\text{Ru}(\text{DMSO})_2\text{Cl}_4]$ ,  $[\text{Na}]\text{trans}-[\text{Ru}(\text{DMSO})_2\text{Cl}_4]$ , and  $[\text{NBu}_4]\text{trans}-[\text{RuCl}_4(\text{DMSO})_2]$  (Bu = *n*-butyl) were synthesized according to the literature methods [27,29].

$[\text{PPh}_4]\text{trans}-[\text{Ru}(\text{DMSO})_2\text{Cl}_4]$  (**1**). Tetraphenylphosphonium chloride (0.34 g, 0.92 mmol) dissolved in 6 mL of  $\text{H}_2\text{O}$  was added to a solution of  $[(\text{DMSO})_2\text{H}]\text{trans}-[\text{Ru}(\text{DMSO})_2\text{Cl}_4]$  (0.34 g, 0.61 mmol) dissolved in 3 mL of  $\text{H}_2\text{O}$ , while stirring. A yellow precipitate formed within minutes. The precipitate was collected by filtration, washed with diethylether and vacuum dried. Yield: 89%. IR ( $\text{cm}^{-1}$ ): 1107s  $\nu(\text{DMSO}-\text{S})$ , 416w  $\nu(\text{Ru}-\text{S})$ , 339, 319s  $\nu(\text{Ru}-\text{Cl})$ .  $^1\text{H}$  NMR ( $\text{CD}_3\text{CN}/\text{ppm}$ ):  $-13.0$  (DMSO-S), 7.95, 7.74 (phenyl protons).

$[\text{PPh}_4]\text{trans}-[\text{Ru}(\text{DMSO})(\text{pz})\text{Cl}_4]$  (**2**).  $[\text{PPh}_4]\text{trans}-[\text{Ru}(\text{DMSO})_2\text{Cl}_4]$  (**1**) (0.30 g, 0.40 mmol) was dissolved in a mixture of 7 mL acetone and 4 mL acetonitrile, while

0.16 g of pyrazine (pyz) (2.0 mmol) was dissolved in 1 mL of acetone. The ruthenium solution was added slowly to the pyrazine solution to form a clear orange mixture. After several hours the product precipitated as orange crystals. The crystals were collected by filtration, washed with cold diethylether and vacuum dried. Yield: 73%. Alternatively, complex **2** can be synthesized from complex **3** by the addition of  $[\text{PPh}_4]\text{Br}$  or  $[\text{PPh}_4]\text{Cl}$  in aqueous solution. IR ( $\text{cm}^{-1}$ ): 1588 (pz), 1108s (DMSO-S), 420m  $\nu(\text{Ru}-\text{S})$ , 342, 328s  $\nu(\text{Ru}-\text{Cl})$ .  $^1\text{H}$  NMR ( $\text{CD}_3\text{CN}/\text{ppm}$ ):  $-12.6$  (br, DMSO-S),  $-5.6$  (vbr, pz  $\text{H}^{2,6}$ ),  $-1.6$  (br, pz  $\text{H}^{3,5}$ ), 7.95, 7.74 (phenyl protons). *Anal. Calc.* for  $\text{C}_{30}\text{H}_{30}\text{Cl}_4\text{N}_2\text{OPSRu}$ : C, 48.6; H, 4.05; N 3.78. Found: C, 48.4; H, 3.84; N, 3.87%.

$[\text{Na}]\text{trans}-[\text{Ru}(\text{DMSO})(\text{pz})\text{Cl}_4] \cdot \text{DMSO}$  (**3**). The synthesis of this compound was similar to that reported [27] with some changes. Pyrazine (80.2 mg, 1.00 mmol) dissolved in 5 mL of acetone was added to a solution of 82.5 mg (0.198 mmol) of  $[\text{Na}]\text{trans}-[\text{Ru}(\text{DMSO})_2\text{Cl}_4]$  dissolved in 2 mL of DMSO. The resulting mixture was filtered and the filtrate was stirred at room temperature for 1.5 h. A 50/50 acetone/diethylether solution (5.0 mL) was added to the reaction mixture followed by an additional 5.0 mL of diethylether. The mixture was then placed at  $4^\circ\text{C}$ . Orange crystals appeared within 48 h. The mother liquor was decanted and the crystals washed with diethylether. Yield: 67%.  $^1\text{H}$  NMR ( $\text{D}_2\text{O}/\text{ppm}$ ):  $-13.9$  (br), (DMSO-S),  $-7.5$  (vbr,  $\text{H}^{3,5}$  pyz),  $-2.1$  (br,  $\text{H}^{2,6}$  pyz). This compound was reported, but the solvate molecules appear different [27].

$[\text{NBu}_4]\text{trans}-[\text{RuCl}_4(\text{DMSO})(\text{bpy})]$  (**4**). 0.63 g of  $[\text{NBu}_4]\text{trans}-[\text{RuCl}_4(\text{DMSO})_2]$  (0.98 mmol) was dissolved in 15 mL of acetone and 0.60 g of 4,4-bipyridine (3.8 mmol) was dissolved in 4 mL of acetone. The ruthenium solution was added to the 4,4-bipyridine solution to form a clear orange solution. After several hours of stirring, the product was precipitated after the addition of 10 mL of cold diethylether. The yellow precipitate was collected by filtration, washed with cold diethylether and vacuum dried. Yield: 86% (0.60 g). IR ( $\text{cm}^{-1}$ ): 1595, 1612w (bpy), 1109s (DMSO-S), 422m  $\nu(\text{Ru}-\text{S})$ , 349, 325s  $\nu(\text{Ru}-\text{Cl})$ .  $^1\text{H}$  NMR (acetone/ppm):  $-12.2$  (br, DMSO-S), 7.5 (br, bpy  $\text{H}^{2,6}$ ), 6.0 (br, bpy  $\text{H}^{3,5}$ ),  $-1.2$  (br, bpy  $\text{H}^{3,5}$ ),  $-6.0$  (vbr, bpy  $\text{H}^{2,6}$ ).

$[\text{PPh}_4]\text{trans}-[\text{RuCl}_4(\text{DMSO})(\text{bpy})]$  (**5**). 0.50 g of  $[\text{PPh}_4]\text{trans}-[\text{RuCl}_4(\text{DMSO})_2]$  (0.68 mmol) was dissolved in 15 mL of  $\text{CH}_2\text{Cl}_2$  and 0.40 g of 4,4-bipyridine (2.6 mmol) was dissolved in 6 mL of  $\text{CH}_2\text{Cl}_2$ . The ruthenium solution was added to the 4,4-bipyridine solution to form a clear orange solution. After several hours of stirring, the product was precipitated after the addition of 10 mL of cold diethylether. The yellow precipitate was collected by filtration, washed with cold diethylether, and vacuum dried. Yield: 82% (0.45 g). IR ( $\text{cm}^{-1}$ ): 1595, 1612w (bpy), 1107s (DMSO-S), 422m  $\nu(\text{Ru}-\text{S})$ , 331s,br  $\nu(\text{Ru}-\text{Cl})$ .  $^1\text{H}$  NMR ( $\text{CDCl}_3/\text{ppm}$ ):  $-12.8$  (br, DMSO-S), 7.5 (br, bpy  $\text{H}^{2,6}$ ), 5.5 (br, bpy  $\text{H}^{3,5}$ ),  $-1.7$  (br, bpy  $\text{H}^{3,5}$ ), 8.06 (br, phenyl protons). *Anal. Calc.* for  $\text{C}_{36}\text{H}_{34}\text{Cl}_4\text{N}_2\text{OPSRu}$ : C, 52.9; H, 4.17; N 3.43. Found: C, 52.6; H, 3.94; N, 3.23%.

$[PPh_4]trans-[RuCl_4(DMSO)(pym)]$  (*pym* = pyrimidine) (**6**). 0.20 g of  $[PPh_4]trans-[RuCl_4(DMSO)_2]$  (0.27 mmol) was dissolved in 5 mL of  $CH_2Cl_2$  and 0.15 g of pyrimidine (0.98 mmol) was dissolved in 1 mL of acetone. The ruthenium solution was added to the pyrimidine solution to form a clear orange solution. After several hours of stirring, the product was precipitated with the addition of 10 mL of diethylether. The yellow precipitate was collected by filtration, washed with diethylether, and vacuum dried. Yield: 67% (0.133 g). IR ( $cm^{-1}$ ): 1585, 1560 (*pym*), 1107s (DMSO–S), 421m  $\nu$ (Ru–S), 339, 324sh  $\nu$ (Ru–Cl).  $^1H$  NMR ( $CD_3CN/ppm$ ): –13.0 (br, DMSO–S), 6.34 (*pym*  $H^4$ ), –0.58 (br, *pym*  $H^5$ ), –1.7 (vbr, *pym*  $H^6$ ), –6.5 (vbr, *pym*  $H^2$ ), 7.96, 7.78 (br, phenyl protons); ( $CDCl_3/ppm$ ): –12.7 (br, DMSO–S), 6.32 (br, *bpy*  $H^4$ ), –0.52 (br,  $H^5$ ), 8.16 (br, phenyl protons). *Anal. Calc.* for  $C_{30}H_{30}Cl_4N_2OPSRu$ : C, 48.6; H, 4.05; N 3.78. Found: C, 48.4; H, 3.78; N, 3.77%.

## 2.2. Crystallographic measurements and structure resolution

The crystallographic measurements of crystals **2** and **3** were done on a Bruker P4 diffractometer using graphite-monochromatized Mo  $K\alpha$  ( $\lambda = 0.71073 \text{ \AA}$ ) radiation. The cell dimensions were determined at room temperature, from a least-squares refinement of the angles  $2\theta$ ,  $\omega$  and  $\chi$  obtained for well-centered reflections. The data collection was made by the  $2\theta/\omega$  scan technique using the XSCANS program [30]. The background time to scan time ratio was 0.5.

Table 1  
Crystallographic data and experimental details

Crystal	<b>2</b>	<b>3</b>
Name	$PPh_4[Ru(DMSO)(pz)Cl_4]$	$Na[Ru(DMSO)(pz)Cl_4] \cdot DMSO$
Chemical formula	$C_{30}H_{30}Cl_4N_2OPRuS$	$C_8H_{16}Cl_4N_2NaO_2RuS_2$
$M_w$	740.46	502.21
Space group	$P2_1/n$ (No. 14)	$P\bar{1}$ (No. 2)
$a$ ( $\text{\AA}$ )	13.161(3)	7.0972(7)
$b$ ( $\text{\AA}$ )	17.070(4)	10.6838(15)
$c$ ( $\text{\AA}$ )	14.826(4)	12.379(2)
$\alpha$ ( $^\circ$ )	90.	91.164(14)
$\beta$ ( $^\circ$ )	104.65(2)	93.48(12)
$\gamma$ ( $^\circ$ )	90.	105.83(11)
Volume ( $\text{\AA}^3$ )	3222.5(14)	900.7(2)
$Z$	4	2
$\rho_{calc}$ ( $g\ cm^{-3}$ )	1.526	1.852
$\mu$ (Mo $K\alpha$ ) ( $mm^{-1}$ )	0.959	1.718
$F(000)$	1500	498
Reflections collected	12656	10499
Observed Reflections ( $I > 2\sigma(I)$ )	4778	4284
$R_1$ ( $I > 2\sigma(I)$ )	0.0327	0.0307
$wR_2$ (all data)	0.0748	0.0770
$S$	1.049	1.023

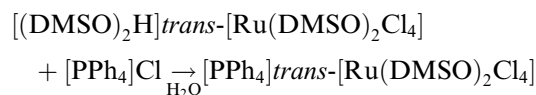
$$R_1 = \sum(|F_o - F_c|) / \sum|F_o|, wR_2 = [\sum(w(F_o^2 - F_c^2)^2) / \sum(w(F_o^2)^2)]^{1/2}.$$

The coordinates of the Pt atom were determined by direct methods and all the other non-hydrogen atoms were found by the usual Fourier methods. The refinement of the structure was done on  $F^2$  by full matrix least-squares analysis. The hydrogen atom positions were fixed in their calculated positions with  $U_{eq} = 1.2 U_{eq}$  (or 1.5 for methyl groups) of the carbon to which they are bonded. Corrections were made for absorption (semi-empirical from psi-scans for **2** and integration for **3**), Lorentz and polarization effects. The calculations were done using the Bruker SHELXTL system [30]. The crystallographic data and details are shown in Table 1.

## 3. Results and discussion

### 3.1. $[PPh_4]trans-[Ru(DMSO)_2Cl_4]$ (**1**)

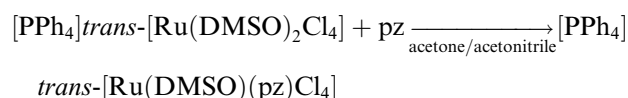
This yellow compound was synthesized from the aqueous reaction of  $[(DMSO)_2H]trans-[Ru(DMSO)_2Cl_4]$  with tetraphenylphosphonium chloride.



The synthesis and characterization of this ionic complex has not been reported yet in the literature, therefore we give a brief description. The IR spectrum of the compound shows a  $\nu$ (S–O) vibration at  $1107\ cm^{-1}$ . Absorption at  $416\ cm^{-1}$  was assigned to the metal stretching vibration  $\nu$ (Ru–S) while those at 339 and  $319\ cm^{-1}$  were attributed to  $\nu$ (Ru–Cl). The NMR spectrum of **1** and all of the complexes reported here show peaks that are characteristic of complexes containing paramagnetic ruthenium(III). Protons close to the paramagnetic center have large line-width (often some peaks are too wide to be observable) and are shifted greatly upfield [31–33]. The peak at –13.0 ppm is assigned to the coordinated DMSO (through the S atom).

### 3.2. $[PPh_4][Ru(DMSO)(pyrazine)Cl_4]$ (**2**)

This new ionic complex was synthesized from the reaction of the bis-DMSO Ru(III) ionic complex **1** with pyrazine (pz) as shown in the following equation:



Alternatively, compound **2** was also synthesized from the aqueous reaction of compound **3** with tetraphenylphosphonium chloride or tetraphenylphosphonium bromide.

The IR spectrum of **2** shows a  $\nu$ (S–O) vibration at  $1108\ cm^{-1}$ , a  $\nu$ (Ru–S) band at  $420\ cm^{-1}$  and  $\nu$ (Ru–Cl) vibrations at 342 and  $328\ cm^{-1}$ . The NMR spectrum shows a peak at –12.6 ppm integrating to six protons assigned to the coordinated DMSO, while the peak at –1.6 ppm integrating to two protons is assigned to the protons ( $H^3$  and  $H^5$ ) on the pyrazine ring. The protons on the pyrazine ring

(H<sup>2</sup> and H<sup>6</sup>) closest to the paramagnetic ruthenium center are seen in a very broad peak at  $-5.6$  ppm (for labeling see Chart 1).

Compound **2** was recrystallized from acetone/diethyl-ether and the crystals were studied by crystallographic methods. The results have shown that the orange crystals consist of discrete complexed anions,  $[\text{Ru}(\text{DMSO})(\text{pz})\text{Cl}_4]^-$  (Fig. 1) and  $[\text{PPh}_4]^+$  cations. The complexed anion is the *trans* isomer and the coordination around the Ru(III) center is octahedral. The bond distances and angles are shown in Table 2. The *cis* angles around the metal vary between  $87.73(7)^\circ$  and  $92.66(3)^\circ$ , while the *trans* angles are between  $177.32(3)^\circ$  and  $179.07(7)^\circ$ . The Ru–Cl bond distances range from  $2.3425(9)$  to  $2.3589(10)$  Å, the Ru–S bond is  $2.2941(9)$  Å and the Ru–N distance is  $2.118(2)$  Å. These values are in agreement with published values found in a few related structures [22,24,27,28,34].

The environment around the S atom in the DMSO ligand is approximately tetrahedral but there are small deformations. The O–S–C angles are larger (ave.  $107.18(17)^\circ$ ) than the C–S–C angle ( $98.77(18)^\circ$ ) as expected. The Ru–S–O angle ( $117.98(10)^\circ$ ) is also larger than the Ru–S–C angles (ave.  $111.95(13)^\circ$ ). The average angle Ru–N–C is  $121.9(2)^\circ$ . The N1–C bond lengths (ave.  $1.332(4)$  Å) are not different from those of N4–C (ave.

$1.328(5)$  Å), but the angles C–N–C are different. The internal ring angle at the metal-bonded N1 atom is larger ( $116.3(3)^\circ$ ) than the angle of the non-bonded N4 atom ( $114.7(3)^\circ$ ) as observed in Pt(II) compounds of the type *cis*- and *trans*-Pt(R<sub>2</sub>SO)(pz)Cl<sub>2</sub> where the bonded angle C2–N1–C6 is slightly larger than the C3–N4–C5 angle [35].

In order to minimize the interactions with the rest of the molecule, the pyrazine ligand is at  $\approx 45^\circ$  to the different Ru square planes. Here, the dihedral angle between the pyrazine and the RuN1S1Cl1Cl3 plane is  $47.65(11)^\circ$ , while it is  $42.36(10)^\circ$  with the RuN1S1Cl2Cl4 plane. In the DMSO ligand, the O atom of DMSO was found almost in the RuS1N1Cl1Cl3 plane, which reduces steric hindrance in the complexed ion, since the larger methyl groups are far from the four *cis* chloro ligands. The torsion angles Cl1–Ru–S–O and Cl3–Ru–S–O are  $-7.14(15)^\circ$  and  $172.94(15)^\circ$ , respectively. In this conformation of the DMSO and pyrazine ligands, the energy of the molecular ion is close to a minimum.

The PPh<sub>4</sub> cations are normal. The average P–C bond distance is  $1.800(3)$  Å with an average C–P–C angle of  $109.48(13)^\circ$ . No H-bonds are expected in this crystal. The ions are held together in the crystal by electrostatic forces and by van der Waals interactions.

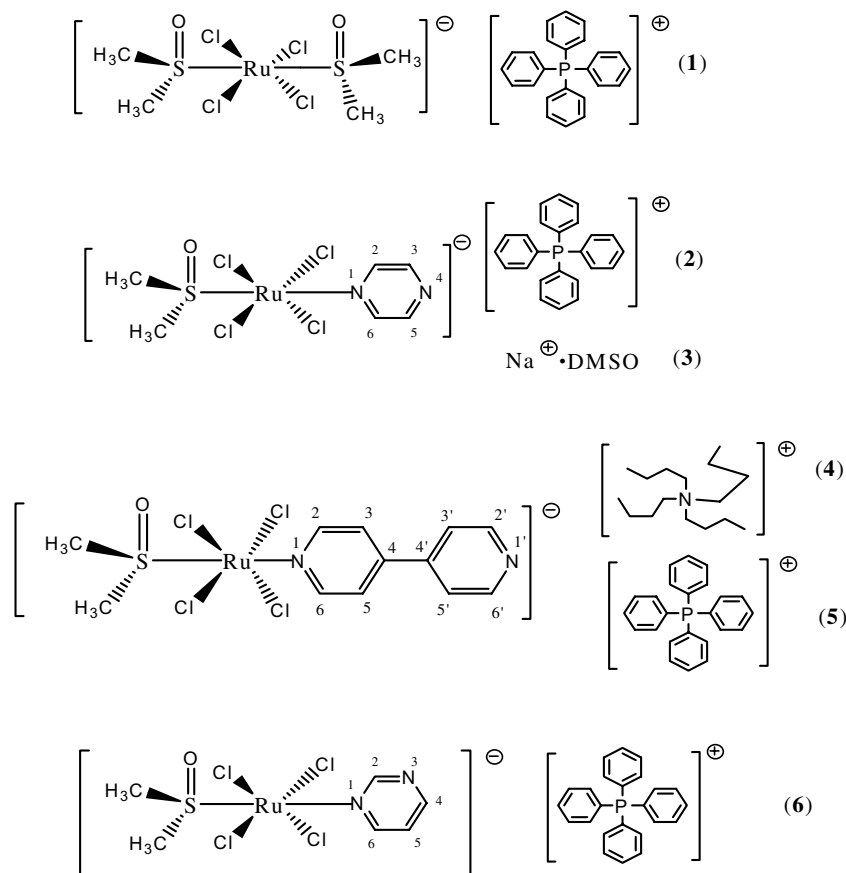


Chart 1. Ruthenium(III) molecular structures.

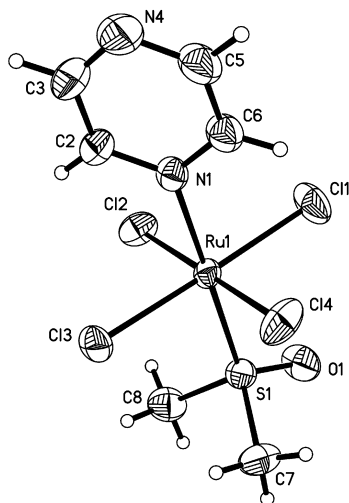
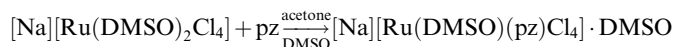


Fig. 1. ORTEP view of the  $[\text{Ru}(\text{DMSO})(\text{pz})\text{Cl}_4]^-$  anion in crystal **2**. Ellipsoids are shown at 40% probability level and the H atoms are of arbitrary size.

### 3.3. $[\text{Na}][\text{Ru}(\text{DMSO})(\text{pyrazine})\text{Cl}_4] \cdot \text{DMSO}$ (**3**)

This compound was synthesized from the reaction of  $[\text{Na}][\text{Ru}(\text{DMSO})_2\text{Cl}_4]$  with pyrazine in acetone and DMSO similar to the procedure already reported.



The orange compound was crystallized in a mixture of acetone and diethylether and the crystals were studied by X-ray diffraction methods. The results have shown that the compound crystallized with a molecule of solvent (DMSO). The reported compound [27], which was not studied by crystallographic methods, contained 1.5 molecule of DMSO and 0.5 molecule of  $\text{H}_2\text{O}$ , although it was crystallized from the same solvents.

Fig. 2 shows the labeling scheme of the asymmetric unit in crystal **3**. The complexed anion is the *trans* isomer and the coordination around the Ru(III) center is octahedral. The bond distances and angles are shown in Table 2. The *cis* angles around the metal vary between  $87.95(3)^\circ$  and  $93.96(3)^\circ$ , while the *trans* angles are between  $176.43(2)^\circ$  and  $177.74(2)^\circ$ . The Ru–Cl bond distances range from 2.3395(8) to 2.3754(7) Å, the Ru–S bond is 2.3027(7) Å and the Ru–N distance is 2.1257(19) Å. These values are very similar to those observed in crystal **2** described above and they are in agreement with published values found in a few related structures [22,24,27,28].

The environment around the bonded S atom in the DMSO ligand is approximately tetrahedral but there are small deformations. The O–S1–C angles are larger (ave.  $106.39(17)^\circ$ ) than the C–S1–C angle ( $100.4(2)^\circ$ ) as expected. The Ru–S–O angle ( $117.73(8)^\circ$ ) is also larger than the Ru–S–C angles (ave.  $112.15(17)^\circ$ ). The average angle Ru–N–C is  $121.64(16)^\circ$ . The N1–C bonds (ave.

Table 2  
Bond distances (Å), bond and torsion angles ( $^\circ$ )

	2	3
Ru–Cl1	2.3425(9)	2.3754(7)
Ru–Cl2	2.3449(9)	2.3458(7)
Ru–Cl3	2.3520(8)	2.3395(8)
Ru–Cl4	2.3589(10)	2.3684(7)
Ru–N1	2.118(2)	2.1257(19)
Ru–S1	2.2941(9)	2.3027(7)
S1–O1	1.468(2)	1.4705(19)
S1–C (ave.)	1.787(3)	1.770(3)
S2–O2		1.496(2)
S2–C (ave.)		1.784(3)
N1–C (ave.)	1.332(4)	1.343(3)
N4–C (ave.)	1.328(5)	1.333(3)
P1–C (ave.)	1.800(3)	
N1–Ru–S1	179.07(7)	177.68(6)
N1–Ru–Cl1	88.27(7)	88.35(6)
N1–Ru–Cl2	90.08(7)	89.98(6)
N1–Ru–Cl3	89.91(7)	89.29(6)
N1–Ru–Cl4	87.73(7)	89.25(6)
S1–Ru–Cl1	92.66(3)	93.96(3)
S1–Ru–Cl2	90.02(4)	89.86(3)
S1–Ru–Cl3	89.16(3)	88.40(3)
S1–Ru–Cl4	92.15(4)	91.04(2)
Cl1–Ru–Cl2	91.08(4)	87.95(3)
Cl1–Ru–Cl3	178.18(3)	177.74(2)
Cl1–Ru–Cl4	90.39(4)	88.55(2)
Cl2–Ru–Cl3	89.00(4)	92.14(3)
Cl2–Ru–Cl4	177.32(3)	176.43(2)
Cl3–Ru–Cl4	89.46(4)	91.34(3)
Ru–N1–C (ave.)	121.4(2)	121.64(16)
Ru–S1–O1	117.98(10)	117.73(8)
Ru–S1–C (ave.)	111.95(13)	112.15(12)
O1–S1–C (ave.)	107.18(17)	106.39(17)
C–S1–C	98.77(18)	100.4(2)
O1–S2–C (ave.)		105.99(15)
C–S2–C		98.49(17)
C2–N1–C6	116.3(3)	116.7(2)
C3–N4–C5	114.7(3)	115.2(2)
C–P–C (ave.)	109.48(13)	
Cl1–Ru–S1–O1	–7.14(15)	–161.74(11) (Cl2)
Cl3–Ru–S1–O1	172.94(15)	21.71(11) (Cl4)
Cl–Ru–N1–C (ave.)	$\approx 45$	$\approx 45$

#### Distances and angles around the Na atom in **3**

Na–O1	2.303(2)	Na–O2	2.324(2)
Na–N4'	2.519(2)	Na–Cl1'	2.7760(13)
Na–Cl4	2.9222(12)	Na–Cl4'	2.8404(13)
O1–Na–O2	92.97(9)	O1–Na–N4'	86.13(8)
O1–Na–Cl1'	175.65(8)	O1–Na–Cl4	76.74(6)
O1–Na–Cl4'	104.86(7)	O2–Na–N4'	92.89(8)
O2–Na–Cl1'	89.89(6)	O2–Na–Cl4	106.54(7)
O2–Na–Cl4'	162.13(7)	N4'–Na–Cl1'	92.00(6)
N4'–Na–Cl4	154.51(7)	N4'–Na–Cl4'	87.33(6)
Cl1'–Na–Cl4	104.10(4)	Cl1'–Na–Cl4'	72.25(3)
Cl4–Na–Cl4'	79.17(3)	Na–N4–C (ave.)	122.08(16)
Na–O1–S1	135.34(13)	Na–O2–S2	124.79(12)
Na'–Cl1–Ru	100.17(3)	Na'–Cl4–Ru	98.55(3)
Na–Cl4–Ru	111.28(3)	Na–Cl4–Na'	100.83(3)

1.343(3) Å) are not very different from the N4–C bonds (ave. 1.333(3) Å), but the angles C–N–C are slightly different. The internal ring angle at the metal-bonded N1 atom is slightly larger ( $116.7(2)^\circ$ ) than the angle of the non-bonded

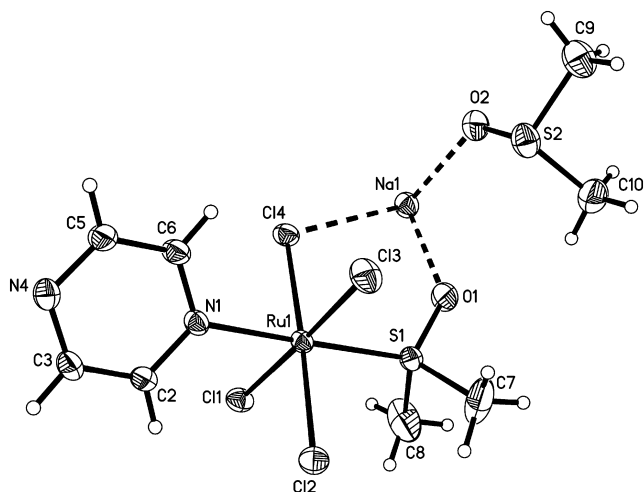


Fig. 2. ORTEP view of  $[\text{Na}][\text{Ru}(\text{DMSO})(\text{pz})\text{Cl}_4] \cdot \text{DMSO}$  (**3**) showing the labelling scheme of the asymmetric unit. Ellipsoids are shown at 40% probability level and the H atoms are of arbitrary size.

N4 atom ( $115.2(2)^\circ$ ), as observed in crystal **2**, which also contains a monodentate pyrazine ligand.

Complex **3** crystallized with a molecule of DMSO which is not bonded to the Ru(III) atom. The S2–O2 bond is longer ( $1.496(2) \text{ \AA}$ ) than the S1–O1 bond distance in crystals **2** and **3** (ave.  $1.469(2) \text{ \AA}$ ) as expected when the S atom is not coordinated to a metal. When the binding site of DMSO is the S atom, the order of the S–O bond increases when compared to the free molecule, while it is reduced if the molecule is bonded to the metal atom through its O atom. The NMR and IR spectra are in agreement with the published data. Only one  $\nu(\text{S–O})$  band was observed at  $1104 \text{ cm}^{-1}$  [27].

The O atom of the bonded DMSO ligand was found close to the RuS1N1Cl2Cl4 plane, which reduces steric hindrance in the complexed anion, since the larger methyl groups are far for the four *cis* chloro ligands. The torsion angles Cl2–Ru–S1–O1 and Cl4–Ru–S1–O1 are  $-161.74(11)^\circ$  and

$21.71(11)^\circ$ , respectively. The plane of pyrazine is located at about  $\approx 45^\circ$  from the two different Ru(III) square planes. The dihedral angle between the pyrazine and the RuN1S1Cl2Cl4 plane is  $41.56(6)^\circ$ , while it is  $48.18(7)^\circ$  with the RuN1S1Cl1Cl4 plane. This conformation of the molecular ion is similar to the one observed in crystal **2** and corresponds approximately to the one of lowest energy.

The environment around the Na atoms was closely examined. There are six atoms in its close environment. The distances and angles are shown in Table 2. The geometry is a distorted octahedron. Three of the close contacts are shown in Fig. 2. The Na–O1 (from bonded DMSO) and Na–O2 (unbonded DMSO) distances are  $2.303(2)$  and  $2.324(2) \text{ \AA}$ , respectively. The Na–Cl4 distance is  $2.9222(12) \text{ \AA}$ . There are three other short contacts with the following: N4' ( $2.519(2) \text{ \AA}$ ), Cl1' ( $2.7760(13) \text{ \AA}$ ), and Cl4' ( $2.8404(13) \text{ \AA}$ ). The chloro ligand Cl4 forms a bridge between two Na atoms, while Cl1 forms a bridge between a Na and a Ru atom. The two other Cl ligands are not involved with the Na atoms. The DMSO ligand forms a bridge between a Ru (through its S atom) atom and a Na (through its O) atom, while the S atom of the second DMSO molecule is free, but its O atom is in the close environment of the Na atom. There are important distortions from the octahedral structure around the Na atom. The *cis* angles vary between  $72.25(3)^\circ$  (Cl'–Na–Cl4') and  $106.54(7)^\circ$  (O2–Na–Cl4), while the *trans* angles are between  $154.51(7)^\circ$  and  $175.65(8)^\circ$ .

The Na atom has a very important role in this structure. It bridges the different complexed ions to form infinite polymeric chains or ribbons parallel to the *b* axis. One of these is shown in Fig. 3. The two ligands Cl2 and Cl3, which are not involved with the Na atoms point towards the outside of the chain, along with S2 and the two C atoms of the free DMSO molecule. Several cycles are formed, ranging from four atoms (Ru, Cl1, Na, Cl4) to seven atoms (Ru, Cl1, Na, Cl4, Na, O1, S1). These neutral ribbons are held together by van der Waals forces. There may be weak  $\pi$ – $\pi$  stacking

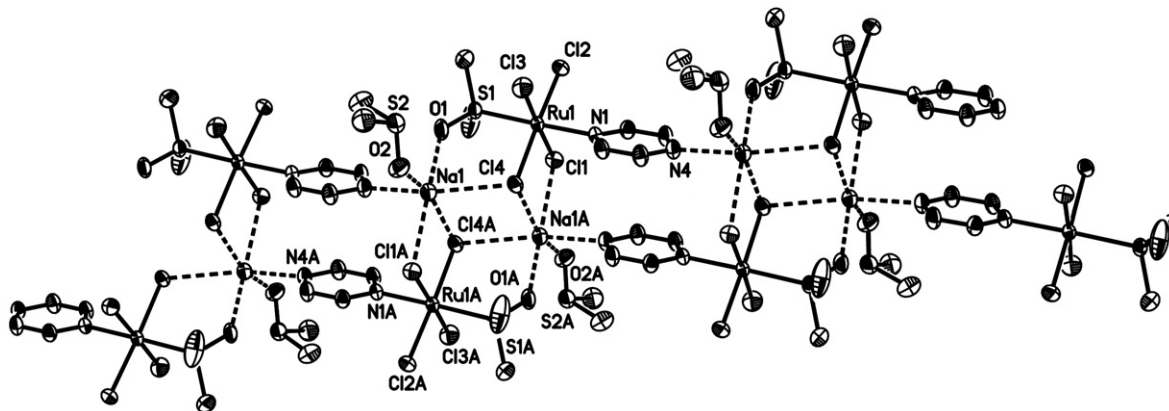


Fig. 3. ORTEP view of a ribbon in compound **3** showing the octahedral environment around the Na atom (---), which bridges the anions  $[\text{Ru}(\text{DMSO})(\text{pz})\text{Cl}_4]^-$ .

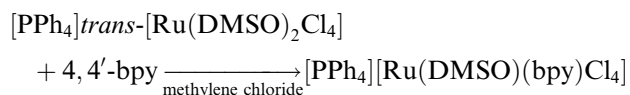
interactions of the pyrazine ligands, as the distance between pyrazine pairs shown in Fig. 3 is 3.548(16) Å [36].

A few related structures were reported with the sodium cation. In  $[\text{Na}][\text{Ru}(\text{DMSO})(\text{NH}_3)\text{Cl}_4] \cdot 2\text{DMSO}$  and  $[\text{Na}][\text{Ru}(\text{DMSO})(\text{Im})\text{Cl}_4] \cdot \text{H}_2\text{O}$ ,  $\text{CH}_3\text{COCH}_3$  [22], the environment around the Na atom is tetrahedral with four Na–O distances between 2.272(4) and 2.489(3) Å. But the long-range arrangement in the crystal was not discussed. A few other related structures containing Na ions were published, but the environment around the Na atom was not considered [27]. In these structures, the role of the Na ions in the architecture, besides its counterion function, was not studied.

In crystal 3, the unbonded DMSO molecule plays also a very important role in the formation of the chains. In a few reported structures containing the same cation, the chains are not formed, but rather shorter oligomers [22] containing two Ru(III) and two Na atoms were produced. For the latter structures, the tetrahedral environment around the Na atoms is formed with four O atoms from DMSO or  $\text{H}_2\text{O}$  molecules.

#### 3.4. $[\text{NBu}_4]\text{trans}[\text{RuCl}_4(\text{DMSO})(\text{bpy})]$ (4) and $[\text{PPh}_4]\text{trans}[\text{RuCl}_4(\text{DMSO})(\text{bpy})]$ (5)

$[\text{PPh}_4]\text{trans}[\text{Ru}(\text{DMSO})(\text{bpy})\text{Cl}_4]$  (5) (bpy = 4,4'-bipyridine) was prepared from  $[\text{PPh}_4]\text{trans}[\text{Ru}(\text{DMSO})_2\text{Cl}_4]$  in methylene chloride as shown in the following equation:

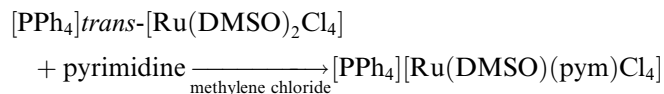


The NMR spectrum of compound 5 showed, along with signals for the tetraphenyl phosphonium cation, several peaks for the protons of the coordinated ligands. The signal at –12.8 ppm is assigned to the coordinated DMSO while the peak at –1.7 ppm is assigned to the protons ( $\text{H}^3$  and  $\text{H}^5$ ) on the coordinated pyridine ring but furthest from the paramagnetic ruthenium(III) center. The protons closest to the ruthenium center ( $\text{H}^2$  and  $\text{H}^6$ , Chart 1) are not observed due to a line-width that is too broad for the peak to be seen. The protons on the second pyridine ring are observed at 5.5 ( $\text{H}^{3'}$  and  $\text{H}^{5'}$ ) and 7.5 ppm ( $\text{H}^{2'}$  and  $\text{H}^{6'}$ ) for the two pairs closer and further from the ruthenium atom, respectively. The IR spectrum of 5 shows a terminal bpy mode at  $1595\text{ cm}^{-1}$  along with a  $\nu(\text{S}-\text{O})$  vibration at  $1107\text{ cm}^{-1}$ , a  $\nu(\text{Ru}-\text{S})$  band at  $422\text{ cm}^{-1}$ , and a  $\nu(\text{Ru}-\text{Cl})$  vibration at  $331\text{ cm}^{-1}$ .

$[\text{NBu}_4]\text{trans}[\text{Ru}(\text{DMSO})(\text{bpy})\text{Cl}_4]$  (4) was prepared similarly to complex 5, however the reaction was done in acetone solution. The NMR and IR spectral characterization and signal assignments were also similar, except in the proton NMR, where all four sets of bpy proton pairs were observed in this case. The protons closest to the ruthenium atom ( $\text{H}^2$  and  $\text{H}^6$ ), unobservable for complex 5 are seen as a very broad peak at –6.0 ppm.

#### 3.5. $[\text{PPh}_4]\text{trans}[\text{Ru}(\text{DMSO})(\text{pym})\text{Cl}_4]$ (6)

$[\text{PPh}_4]\text{trans}[\text{Ru}(\text{DMSO})(\text{pym})\text{Cl}_4]$  (6) was prepared from  $[\text{PPh}_4]\text{trans}[\text{Ru}(\text{DMSO})_2\text{Cl}_4]$  in methylene chloride as shown in the following equation:



The NMR spectrum of compound 6 in acetonitrile solution showed, along with signals for the tetraphenylphosphonium cation, five peaks for the protons of the coordinated ligands. The signal at –13.0 ppm is assigned to the coordinated DMSO as expected. There are four peaks seen for the pyrimidine ligand as each proton is unique in this case due to the loss of symmetry in the ligand once it has coordinated. The peak at 6.34 ppm has the narrowest line-width and is therefore assigned to the proton furthest from the paramagnetic center,  $\text{H}^4$  [31]. The peak at –0.58 ppm is assigned to the  $\text{H}^5$  proton similar to complex 3. Two very broad peaks are observed at –1.7 and –6.5 ppm and are assigned to  $\text{H}^6$  and  $\text{H}^2$ , respectively, those closest to the paramagnetic ruthenium center. In chloroform solution the peaks were observed at 6.32, –0.52, and –12.7 for the  $\text{H}^4$ ,  $\text{H}^5$ , and DMSO protons, respectively. The  $\text{H}^2$  and  $\text{H}^6$  protons were too broad to be seen. The IR spectrum of 6 shows a terminal pym mode at  $1585\text{ cm}^{-1}$  along with a  $\nu(\text{S}-\text{O})$  vibration at  $1107\text{ cm}^{-1}$ , a  $\nu(\text{Ru}-\text{S})$  band at  $421\text{ cm}^{-1}$ , and  $\nu(\text{Ru}-\text{Cl})$  vibrations at 339 and  $324\text{ cm}^{-1}$ .

## 4. Conclusion

A library search in the Cambridge data file has revealed no Ru complexes containing both a sulfoxide and a monodentate pyrazine ligand. The two structures are also the first examples of Ru(III) compounds containing a monodentate pyrazine ligand. Three structures containing the pyrazine ligand bridging two Ru(III) atoms were found. These are the symmetric dimers  $\text{Na}[(\text{DMSO})\text{Cl}_4\text{Ru}(\mu\text{-pz})\text{RuCl}_4(\text{DMSO})] \cdot \text{H}_2\text{O} \cdot \text{DMSO}$  [27] and  $(\text{TMSO})_2\text{H}[(\text{TMSO})\text{Cl}_4\text{Ru}(\mu\text{-pz})\text{RuCl}_4(\text{TMSO})] \cdot \text{CH}_3\text{COCH}_3$  (where TMSO = tetramethylenesulfoxide) [34], and the unsymmetrical  $\text{NH}_4-[(\text{DMSO})\text{Cl}_4\text{Ru}(\mu\text{-pz})\text{RuCl}_3(\text{S}-\text{DMSO})(\text{O}-\text{DMSO})] \cdot \text{CH}_3\text{-OH}$  dimer [28]. It seems that pyrazine usually function as a bridging ligand and it is more difficult to prepare complexes containing monodentate pyrazine ligands. In the preparation of these types of complexes, the potential bridging ligand was added in a large excess, in order to reduce the formation of pyrazine-bridged oligomeric species. The same is true for the bipyridine and pyrimidine complexes.

The use of cations like  $\text{PPh}_4^+$  or  $\text{NR}_4^+$  which do not form H-bonds or other strong electrostatic attractions like alkali metals should prevent the formation of infinite chains or other materials with extended structures. In the few published structures containing Na cations with a tetrahedral environment, small oligomers are formed [22]. In the case of crystal 3, the  $\text{Na}^+$  cations have an octahedral

environment and it can form bridges between the Ru(III) complexed anions to form a 1D extended structure. It might be interesting to replace the Na atom by a larger metal like Ba, which could accept a larger environment, for example, a coordination number of 8 and form multidimensional (2D or 3D) materials. The formation of such species is an area of current interest in supramolecular chemistry. The study of multidimensional compounds is important in material science, especially for paramagnetic species.

### Acknowledgements

The authors are grateful to the Natural Science and Engineering Research Council of Canada for financial support. We also thank Orgometa, Skylar Ferrara, and Bard College.

### Appendix A. Supplementary material

CCDC 637826 and 637827 contain the supplementary crystallographic data for this paper. These data can be obtained free of charge via <http://www.ccdc.cam.ac.uk/conts/retrieving.html>, or from the Cambridge Crystallographic Data Centre, 12 Union Road, Cambridge CB2 1EZ, UK; fax: (+44) 1223-336-033; or e-mail: [deposit@ccdc.cam.ac.uk](mailto:deposit@ccdc.cam.ac.uk). Supplementary data associated with this article can be found, in the online version, at [doi:10.1016/j.poly.2007.03.041](https://doi.org/10.1016/j.poly.2007.03.041).

### References

- [1] N. Farrell, *Transition Metal Complexes as Drugs and Chemotherapeutic Agents*, Kluwer, Dordrecht, 1989, pp. 44–46.
- [2] P.J. O'Dwyer, J.P. Stevenson, S.W. Johnson, Clinical status of cisplatin, carboplatin, and other platinum-based antitumor drugs, in: B. Lippert (Ed.), *Cisplatin: Chemistry and Biochemistry of a Leading Anticancer Drug*, Verlag, Zurich, Helvetica Chimica Acta (1999) 31–72.
- [3] C.X. Zhang, S.J. Lippard, *Curr. Opin. Chem. Biol.* 7 (2003) 481.
- [4] E.R. Jamieson, S.J. Lippard, *Chem. Rev.* 99 (1999) 2467.
- [5] Z. Suo, S.J. Lippard, K.A. Johnson, *Biochemistry* 38 (1999) 715.
- [6] S. Komeda, G.V. Kalayda, M. Lutz, A.L. Spek, Y. Yamanaka, T. Sato, M. Chikuma, *J. Med. Chem.* 46 (2003) 1210.
- [7] S. Komeda, M. Lutz, A.L. Spek, M. Chikuma, *J. Reedijk, Inorg. Chem.* 39 (2000) 4230.
- [8] S. van Zutphen, E. Pantoja, R. Soriano, C. Soro, D.M. Tooke, A.L. Spek, H. den Dulk, J. Brouwer, J. Reedijk, *Dalton Trans.* (2006) 1020.
- [9] V. Brabec, O. Novakova, *Drug Resist. Updat.* 9 (2006) 111.
- [10] E. Alessio, G. Mestroni, A. Bergamo, G. Sava, *Met. Ions Biol. Syst.* 42 (2004) 323.
- [11] I. Kostova, *Curr. Med. Chem.* 13 (2006) 1085.
- [12] M.J. Clarke, in: A. Sigel, H. Sigel (Eds.), *Metal Ions in Biological Systems*, Marcel Dekker, New York, 1979, pp. 231–283.
- [13] E. Alessio, G. Balducci, M. Calligaris, G. Casta, W. Attia, G. Mestroni, *Inorg. Chem.* 30 (1991) 609.
- [14] G. Mestroni, E. Alessio, G. Sava, International Patent PCT C 07F 15/00, A61K 31/28, WO 98/00431, 1998.
- [15] C.G. Hartinger, S. Zorbas-Seifried, M.A. Jakupec, B. Kynast, H. Zorbas, B.K. Keppler, *J. Inorg. Biochem.* 100 (2006) 891.
- [16] M. Cocchietto, G. Sava, *Pharmacol. Toxicol.* 87 (2000) 193.
- [17] S. Zorzet, A. Sorc, C. Casarsa, M. Cocchietto, G. Sava, *Met.-Based Drugs* 8 (2001) 1.
- [18] G. Sava, A. Bergamo, M. Cocchietto, *Clin. Cancer Res.* 6 (2000) 4566.
- [19] G. Sava, I. Capozzi, V. Clerici, G. Gagliardi, E. Alessio, G. Mestroni, *Clin. Exp. Metastasis* 16 (1998) 371.
- [20] M.J. Clarke, *Coord. Chem. Rev.* 236 (2003) 209.
- [21] J.M. Rademaker-Lakhai, D. Van den Bongard, D. Pluim, J.H. Beijnen, J.H. Schellens, *Clin. Cancer Res.* 10 (2004) 3717.
- [22] E. Alessio, G. Balducci, G. Lutman, G. Mestroni, M. Calligaris, W.M. Attia, *Inorg. Chim. Acta* 203 (1993) 205.
- [23] P. Mura, M. Camalli, L. Messori, F. Piccioli, P. Zanello, M. Corsini, *Inorg. Chem.* 43 (2004) 3863.
- [24] I. Turel, M. Pecanac, A. Golobic, E. Alessio, B. Serli, A. Bergamo, G. Sava, *J. Inorg. Biochem.* 98 (2004) 393.
- [25] Q.A. de Paula, A.A. Batista, O.R. Nascimento, A.J. da Costa-Filho, M.S. Schultz, M.R. Bonfadini, G. Oliva, *J. Braz. Chem. Soc.* 11 (2000) 530.
- [26] E. Reisner, V.B. Arion, M.F.C. Guedes da Silva, R. Lichtenecker, A. Eichinger, B.K. Keppler, V. Kukushkin, A.J.L. Pombeiro, *Inorg. Chem.* 43 (2004) 7083.
- [27] E. Alessio, G. Mestroni, S. Geremia, M. Calligaris, E. Iengo, *Dalton Trans.* (1999) 3361.
- [28] B. Serli, E. Iengo, T. Gianferrara, E. Zangrando, E. Alessio, *Met.-Based Drugs* 8 (2001) 9–18.
- [29] E. Alessio, M. Bolle, B. Milani, G. Mestroni, P. Faleschini, S. Geremia, M. Calligaris, *Inorg. Chem.* 34 (1995) 4716.
- [30] XSCANS and SHELXTL Programs (PC, version 5), Bruker Analytical X-ray Systems, Madison, WI, 1995.
- [31] C. Anderson, A.L. Beauchamp, *Inorg. Chem.* 34 (1995) 6065.
- [32] C. Anderson, A.L. Beauchamp, *Can. J. Chem.* 73 (1995) 471.
- [33] C. Anderson, *Can. J. Chem.* 79 (2001) 1477.
- [34] R.S. Srivastava, F.R. Fronczek, L.M. Romero, *Inorg. Chim. Acta* 357 (2004) 2410.
- [35] F.D. Rochon, J.R.L. Priqueler, *Can. J. Chem.* 82 (2004) 649.
- [36] W. Lu, M.C.W. Chan, K. Cheung, Chi-Ming Che, *Organometallics* (2001) 2477.